Volume: 15 Issue: 03 Pages: 5924– 5930 (2023) ISSN: 0975-0290

Angularly Stable Band Stop FSS Loaded MIMO Antenna with Enhanced Gain and Low Mutual Coupling

Habib Ullah
College of Electronics and Information Engineering, Nanjing University of Aeronautics and Astronautics, Nanjing, China.
Email: habibtelecom209@gmail.com
Qunsheng Cao*
College of Electronics and Information Engineering, Nanjing University of Aeronautics and Astronautics, Nanjing, China.
Email: qunsheng@nuaa.edu.cn
Ijaz Khan
School of Electronics and Information Engineering, Harbin Institute of Technology Harbin, 150001, China.
Email: khanijaz@stu.hit.edu.cn
Inam Ullah
Department of Computer Engineering, Gachon University, Seongnam, Sujeong-gu 13120, Republic of Korea.
Email: inam@gachon.ac.kr
Imran Khan
School of Information and Communication, Guilin University of Electronic Technology Guilin, China.
Email: imrannchu@outlook.com
Saeed Ur Rahman
School of Electronic Engineering, Xidian University, Xi'an, Shaanxi, China.
Email: saeed@xidian.edu.cn

----------ABSTRACT----------

This study investigates the use of a slotted patch MIMO antenna to enhance isolation and gain. Two radiators connected by a network of frequency-selective surfaces (FSS) make up the MIMO antenna design. These antenna components are constructed on an FR-4 substrate and are surrounded by FSS units optimised for X-band frequencies. The suggested MIMO antenna is 65 mm in width, 45 mm in length, and 1.6 mm in height. The main objective of using FSS is to enhance both isolation and gain. The FSS unit cells operate at frequencies ranging from 7 to 9 GHz and have exceptional stability throughout polarisation incidence angles. The FSS-loaded antenna has a bandwidth of 8.0 to 8.55 GHz, a peak gain of 6.5 dB, and a MIMO isolation of greater than -20 dB. Furthermore, the research evaluates the MIMO antenna's performance in terms of diversity gain (DG), efficiency, and envelope correlation coefficient (ECC), demonstrating better results when compared to current state-of-the-art approaches.

Keywords - **FSS; Gain Enhancement; ECC; Diversity Gain; MIMO Antenna.**

Date of Submission: August 29, 2023 Date of Acceptance: October 02, 2023

1. INTRODUCTION

The Microstrip patch antennas (MPAs) have received a lot of interest recently for high-frequency data transfer in a variety of applications. They are popular because of their lightweight design, low cost, and ease of manufacture. Their huge size, however, limits their use in MIMO antenna systems. Although classic MPAs may be used in 5G networks, their small size generally results in limited bandwidth [1]. With the advent of 5G networks, cutting-edge technologies such as virtual reality, smart homes, telemedicine, and the Internet of Vehicles (IoV) will have seamless connections. MIMO antennas are critical for transmitting and receiving numerous data streams inside the same radio network in today's communication landscape [2].

MIMO antennas are an important component in modern wireless communication networks because they minimise interference and boost connection quality and channel capacity without requiring more bandwidth. MIMO antenna design is a significant problem because electromagnetic wave interactions between nearby components can impact antenna parameters such as bandwidth, gain improvement, and radiation pattern [3]. The MIMO antenna system is an attractive field of study that might be used to improve the range and dependability of Wi-Fi LAN, Bluetooth, PDAs, DCS, WLAN, and UMTs. It is also critical for the adoption of next-generation wireless technology. Surface wave and near-field effects produce coupling between antenna components, which has an immediate impact on the array's presentation. As a result, mutual coupling cannot be ignored in many MIMO antenna applications [4, 5]. It is difficult to overcome the mutual coupling problem between antenna components using baseband methods and signal processing. A minimum spacing between neighbouring patches is essential to limit mutual coupling [6]. To address this issue, several strategies for minimising mutual coupling have been investigated, including the stub loading technique [7]. DGS [8, 9], EBG [9, 10], neutralization lines [11], resonator structures [12], slots [13], and metamaterial [14] are all examples of defective ground structures. Antennas with substrates [15], superstrates [16, 17], reflecting surfaces [16, 17, 18, 19, 20], and metamaterials [21] have all been described as ways to improve the gain of microstrip antennas. FSSs are currently mostly two-dimensional arrays of dielectric patches or aperture arrays within a metallic screen that provide the necessary filtering [22]. Another FSS made entirely of dielectrics is suitable for wideband near-field correction, beam scanning, and other high-bandwidth applications [23, 24]. FSS has been studied for nearly 50 years. The FSS may be utilised to increase patch antenna

Volume: 15 Issue: 03 Pages: 5924– 5930 (2023) ISSN: 0975-0290

gain and directivity. FSS are periodic arrays made up of conductive patches or aperture components that reflect or transmit electromagnetic waves depending on their frequency. They function as spatial filters that enable electromagnetic waves to flow through or reflect back. They are often utilised as antenna reflectors [25], Radom [26], electromagnetic absorbers [27], radar cross-section reduction components [28], and artificial magnetic conductors [29]. Because they can stop or let through a certain frequency range. One ongoing problem is decreasing stray bands while increasing antenna gain. Several methods for enhancing gain in MIMO antennas have been investigated. A modern MTM-based superstructure is investigated in [30] for MIMO system gain and isolation enhancements. The antenna in [31] is made up of two semicircular, annular, and rectangular microstrip that are meant to boost gain with the use of a parasitic element and DGS. By combining three pairs of MTM arrays, [32] creates a symmetrical dual-beam end-fire bowtie antenna with a gain increase for 5G MIMO applications. [33] Introduces a single-layer SIW corrugated technique that is later used as the core component of two high gain, low mutual coupling Ka-band MIMO antennas. The antenna structure in [34] is massive and difficult to produce, with two sets of four-element antenna arrays on top and a unique MTM design on the ground plane that enhances gain, bandwidth, and mutual coupling. The slot is placed between the microstrip patch antenna components, minimising mutual coupling and enhancing gain [35]. A ring and a circular parasitic antenna with an air gap were added to a typical circular patch MIMO antenna in [36] to improve its bandwidth and gain. An array antenna decoupling surface and an H-shape DGS were employed to increase the MC in densely packed dual-band MIMO antennas [37]. In [38], a tri-port small antenna with gain augmentation is presented and installed on a hybrid metasurface (MS).

This paper describes a rectangular slotted patch MIMO antenna with high isolation and a 14.5 mm edge-to-edge distance. The antenna operates in the frequency range of 8.15 to 8.55 GHz, providing a well-known frequency standard for X-band applications. MIMO antennas are made up of two rectangular slotted patches that emit signals, as well as an FSS component. The FSS components are arranged in a periodic pattern around the two patches to increase antenna gain and reduce interference between them. The antenna is designed, simulated, and optimised using computer simulation technology (CST). The performance of the antenna is examined using both modelling and measurement, and the results are compared to determine its efficacy.

2. ANALYSIS AND DESIGN

2.1 FSS Design

Figures 1 (a) and (b) show the intended structure of the provided FSS unit cell. The frequency range of the FSS is 7.0 to 9.0 GHz. In the MIMO antenna design, the FSS is incorporated into the same substrate as the patch. The FR4 substrate has a height of 1.6 mm and a dielectric constant of 4.4. CST Microwave Studio is used to do the simulations. The FSS unit cells are tightly spaced to produce a transmission coefficient (S12) of less than -10 dB over the full frequency range. LS = 2, WP= 0.5, WS = 0.5, rp = 3.5,

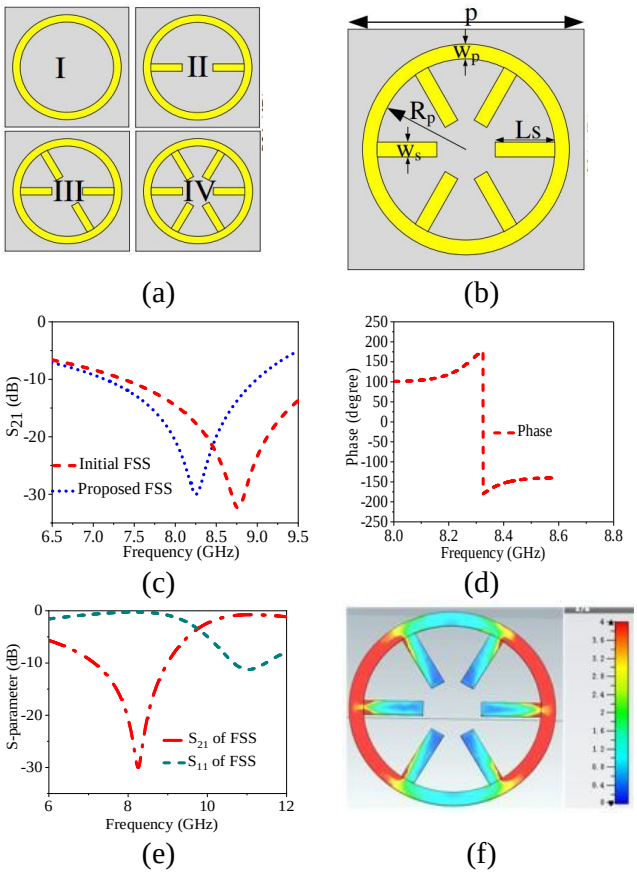

Figure 1 (a) Structure of initial and (b) proposed FSS unit cell and (c) its simulated S-parameter|S21| (d) phase response and (e) S-parameter |S11| and S-parameter |S21| and (f) simulated surface current distribution.

and p = 8.1 are the millimeter dimensions of the proposed unit cell. The transmission coefficient (S21) and reflection phase of the FSS unit cell are shown in Figures 1c and 1d. These data show the proposed FSS operating as a band-stop filter in the frequency range 7–9 GHz, with a transmission coefficient (S21) magnitude of 10 dB. The FSS reflection phase drops linearly with frequency and approaches zero at 8.4 GHz. The suggested FSS presents a linear reflection phase throughout a frequency range of 7 to 9 GHz. Figure 1(c) depicts the suggested FSS's two-stage evolution and transmission coefficient.

Design 1 fundamentally resonates at 8.4 GHz. Design 2 is constructed by adding a stub to the circular resonator, as illustrated in Figure 1(e). The proposed FSS unit cell resonates mostly around 8.8 GHz. Furthermore, a rectangular stub is put into the circular ring to shift the intended frequency towards lower resonance. At 8.4 GHz, to better understand the structure's reaction. The surface current distribution of the investigated antenna is displayed in Figure 1(f). The observation demonstrates that the metallic patch operates at the same frequency as the surrounding air, resulting in a concentrated surface current. This increased current density creates significant surface reflections, lowering transmission efficiency at that frequency.

Volume: 15 Issue: 03 Pages: 5924– 5930 (2023) ISSN: 0975-0290

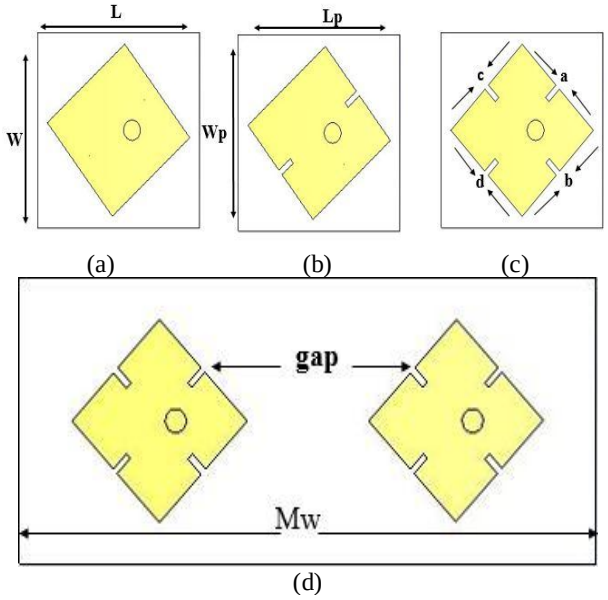

Figure 2 Design steps of proposed antenna (a) step-1 (b) step-2 (c) proposed antenna and (d) Schematic view of the proposed MIMO antenna

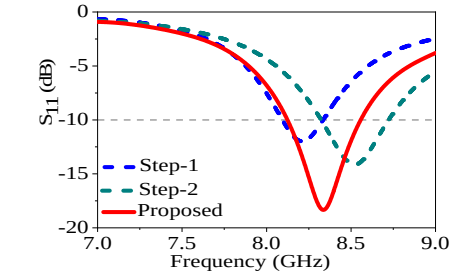

(e)

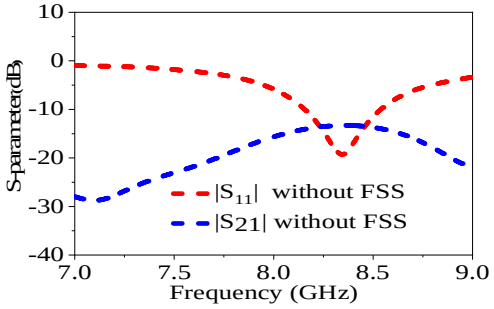

(f)

Figure 2 (a) |S11| and |S21| of MIMO antenna without FSS. [MW =40; gap =14.5. (unit = mm)], (b) Simulated |S11| of different shapes of a single antenna. [L = 12; W =12; a =0.36; b =0.36; c =1.10; d = 1.10. (Unit = mm).

2.2 Antenna design

As shown in Figures 2 (a)–(c), this section develops a basic rectangular slotted patch antenna for X-band applications. As shown in Figure 2(a), the traditional microstrip patch antenna is formed of a rectangular patch and FR-4 as a dielectric substrate with a relative permittivity of 4.4 and tan = 0.025; the thickness is 1.6 mm; and the outside

Dimension is W L = 12.12 mm2. During the second phase of antenna design, a square slot is etched out from the edges, as shown in Figure 2 (b). Figure 2 (d) depicts the simulation results, which clearly show that the resonance frequency has moved to a higher frequency. The suggested design currently has a resonance frequency of 8.4 GHz.

3. PROPOSED MIMO ANTENNA ANALYSIS

3.1 Design of MIMO antenna

Figure 3 (a) shows the suggested slotted patch MIMO antenna system design. These antenna components evolved from the fundamental rectangular patch antenna. The suggested MIMO antenna's exact dimensions are derived using the well-established transmission line theory. The effective resonant length (Ls) and width (Ws) corresponding To a particular resonant Frequency (fr) may be calculated using this theory [41].

$$L_{re} = \frac{c}{2f_r\sqrt{\frac{\varepsilon_r+1}{2}+\frac{\varepsilon_r-1}{2}(1+12\frac{h}{W})^{0.5}}} - 2\Delta L$$

$$W = \frac{1}{2f_r\sqrt{\mu_o\varepsilon_o}}\sqrt{\frac{2}{\varepsilon_r+1}}$$

The total dimensions of a MIMO antenna are 20401.6 mm3, which is less than the size of conventional antennas. On a 1.6 mm thick FR-4 substrate, two radiating patches with slots are constructed. The width and length of the radiators are 7.5 and 7.5 mm, respectively. The substrate is said to be supported by a common ground plane. Initially, basic rectangular patch antenna components operating at 8.4 GHz with mutual coupling (S21) of 16 dB were created. The magnitudes of |S11| and |S21| for the MIMO antenna without Frequency Selective Surface (FSS) are shown in Figure 2 (f). Slots are added to the rectangular patch MIMO antenna to increase its S11 performance. A low mutual coupling is noticed by keeping a spacing of "gap" between the two patches.

3.2 MIMO antenna using FSS

Figures 3 (a) demonstrate the MIMO antenna design with rectangular slotted patches and FSS integration. The antenna elements are two-port slotted patches printed on a rectangular substrate measuring 6545 mm2. The antenna is supplied from two different ports through two 50 SMA connections. The top surface of the substrate is printed with rectangular slotted patches and FSS components. To optimise the antenna's performance, the FSS components are placed at regular intervals around the patches, with a separation distance specified by "c." Impedance matching (S11)

Over the intended resonant frequency band is achieved, indicating satisfactory performance. Furthermore, the impedance matching is successfully retained after loading FSS units around the antenna. Figure 3 (b) and (c) depict the current distribution at 8.4 GHz in the presence and absence of FSS elements. When one antenna (the right side) is activated and the other antenna is terminated with 50 impedances, the patches obtain significant mutual coupling because the current is intimately coupled to other radiators without FSS components, as illustrated in Figure 3(b). The placement of the FSS components, as illustrated in Figure 3 (c), results in a significant drop in current density between the two radiating patches, resulting in increased

Volume: 15 Issue: 03 Pages: 5924– 5930 (2023) ISSN: 0975-0290

performance. As a result, these evaluations aid in determining the best location of FSS components for

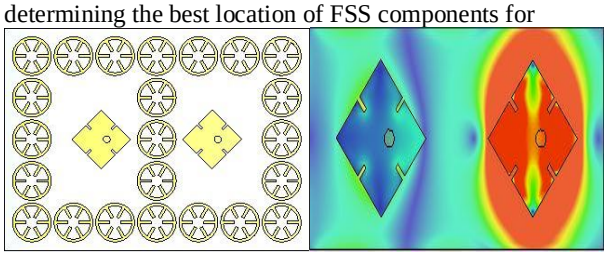

(a) (b)

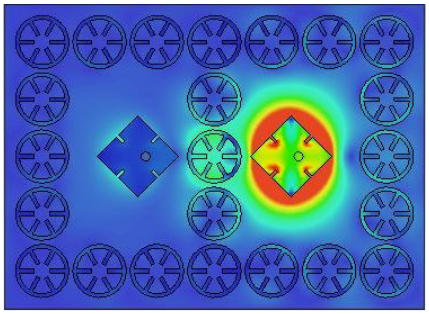

(c)

Figure 3 (a) Schematic view of MIMO antenna using FSSS; and (b) Simulated surface current distribution without FSS and (c) with FSS.

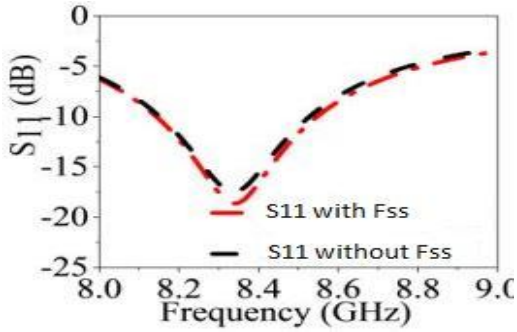

(a)

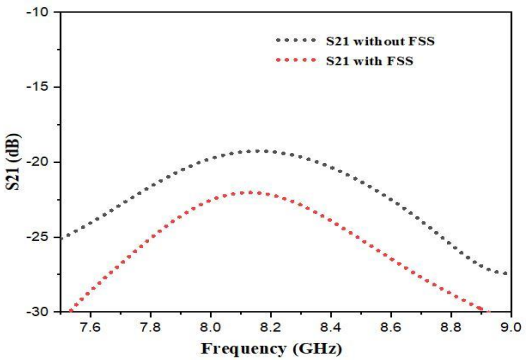

(b)

Figure 4 (a) Simulated S11 (b) Simulated S21

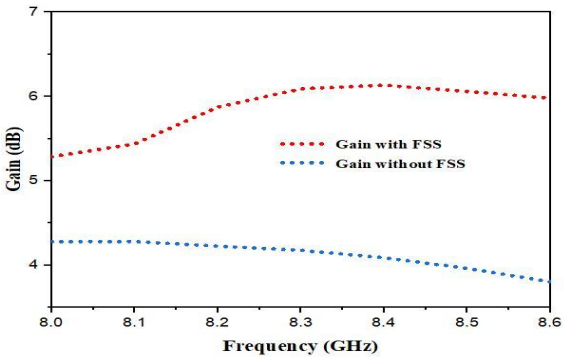

(a)

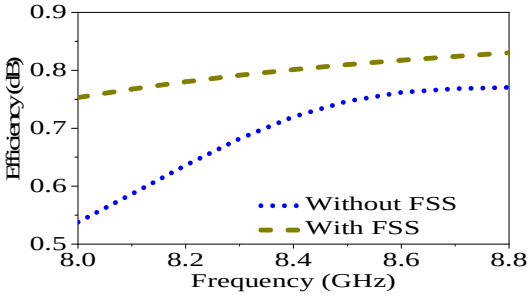

(b)

Figure 5 (a) Simulated Gain with and without FSS; and (b) Simulated Efficiency with and without FSS.

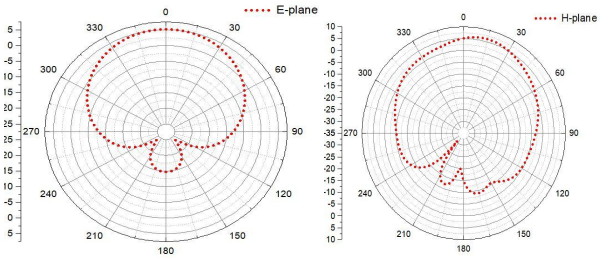

(a) (b)

Figure 6 (a) Simulated E-plane and (b) Simulated H-plane.

Improved patch isolation. The introduction of FSS components between the two patches inhibits current flow to the other side, effectively minimizing coupling between the patches. Furthermore, the isolation, measured by S21, is less than -20 dB after loading the FSS during the two rectangular patches. Figures 4 (a)–(b) show the S11 and S21 of the FSS-based antenna before and after the FSS is included. The proposed MIMO antenna's simulated S11 show good agreement. The simulated gains for the two antennas are also shown in Figure 5 (a). At a frequency of 8.4 GHz, the MIMO antenna has a gain increase of up to 2.5 dB. Figure 5(a) shows the antenna gain with FSS components and without them. Without FSS, the antenna has a gain of 4 dB. With FSS, the gain goes up to 6.25 dB because the aperture's efficiency is increased. When FSS units are put on top of a MIMO antenna, surface current is redistributed, and energy flow from the transmitting element to the antenna surface is enhanced. Because of this, a MIMO antenna with loaded FSS units has a higher aperture efficiency than one

Volume: 15 Issue: 03 Pages: 5924– 5930 (2023) ISSN: 0975-0290

without FSS units. The FSS units around the patch antenna on the right side get more power. When an FSS is used in a MIMO antenna, the gain goes up by a lot.

Based on the results of the study, the increase in gain is caused by the coherent superposition of the energy that the FSS unit cells and patches give off. Figure 5 (b) displays the antenna's radiation efficiency, which is around 77% after accounting for the FSS. Figures 6 (a) (b) depict actual and simulated radiation patterns for the MIMO antenna, respectively, to aid in further analysis. The MIMO antenna with the loaded FSS has a more focused radiation pattern than the MIMO antenna without the loaded FSS, according to the results obtained.

Based on the results of the study, the increase in gain is caused by the coherent superposition of the energy that the FSS unit cells and patches give off. Figure 5 (b) displays the antenna's radiation efficiency, which is around 77% after accounting for the FSS. Figures 6 (a) and (b) depict actual and simulated radiation patterns for the MIMO antenna, respectively, to aid in further analysis. The MIMO antenna with the loaded FSS has a more focused radiation pattern than the MIMO antenna without the loaded FSS, according to the results obtained.

4. DIVERSITY PERFORMANCE OF PROPOSED ANTENNA

Standard system parameters such as the envelope correlation coefficient (ECC) and diversity gain (DG) are used to assess the performance of the MIMO antenna. The antenna's different performances are estimated using the CST Microwave Studio. The next section goes into detail and provides information on these factors.

4.1 Envelope correlation coefficient

The Envelope Correlation Coefficient (ECC) is an important measurement for analysing the performance of MIMO systems. As illustrated in Figure 7 (a), the ECC is utilised to assess the diversity performance of the proposed antenna. The ECC represents the correlation between the received signals from the antenna. It may be estimated using the 3D far-field emission patterns or scattering characteristics of the antenna. It is crucial to note that predicting ECC values for lossy antennas exclusively based on S-parameters is inefficient and frequently leads to an underestimation of the real needs. Equation (3) calculates ECC for a two-port MIMO system while accounting for S-parameters and radiation efficiency [39].

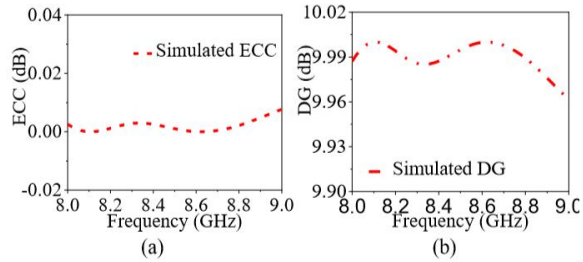

Figure 3 (a) Simulated envelope correlation coefficient and (b) diversity gain.

$$ECC = \frac{|S11 \times S12 + S21 \times S22|}{(1 - |S11|^2) - |S21|^2 (1 - |S21|^2 - |S22|^2)}$$

The ECC, which shows the correlation of the provided antenna, is seen in Figure 7 (a). To achieve optimal MIMO performance, the ECC should be smaller than 0.5 [40]. Figure 7 (a) shows a small correlation between two antennas, with a simulated ECC value continuously less than 0.001 over the full working frequency range. As the ECC value is less than 0.5, this discovery implies that the MIMO antenna has significant pattern variety.

4.2 Diversity Gain

The Diversity Gain (DG) is used in wireless networks to determine the efficiency and dependability of MIMO antennas. It is often accomplished by receiving several broadcast streams over separate channel pathways. As a result, the MIMO antenna should have a high DG, ideally more than 10 dB, within the specified frequency range, as illustrated in Figure 7 (b). Equation (4) may be used to determine the DG, with the ECC value as one of the factors [42].

$$DG = 100 \times \sqrt{1 - (ECC)^2}$$

Table 1 compares the proposed MIMO antenna's performance to that of previously published studies in the literature, with emphasis on the antenna's size, isolation, and high gain. The suggested MIMO antenna has a high gain, a small size, and enough isolation between its radiators. The comparison covers a wide range of topics, including total antenna volume, isolation, mutual coupling reduction, and gain improvement strategies. Table 1 shows that the antenna [16] achieves high gain but has a narrow bandwidth, a two-layer design, and is much bigger in size than the suggested antennas [17, 18], which are likewise larger in size. Compared to the supplied antenna, the antenna [15] is smaller in size but has a two-layer structure and a lesser gain. The suggested design stands out because it uses a single substrate, as opposed to existing antenna designs that use numerous substrates, as shown in Table 1. While alternate approaches may improve antenna gain, they frequently increase complexity, have a bigger footprint, and may have an influence on other characteristics like radiation pattern and efficiency. As a result of its complexity, the antenna's overall cost may increase. The antenna and reflector in this study are constructed on the same substrate, reducing space requirements, and enhancing radiation performance.

5. CONCLUSION

The aim of this study is to present a single-band slotted patch MIMO antenna that improves isolation and gain. The MIMO antenna has a straightforward design with small dimensions of 65 x 45 mm2 and a 14.5 mm gap between the two patches. A unique technique employing an angularly stable band stop FSS is used to boost gain and eliminate mutual coupling. Patch antennas benefit from the use of

Volume: 15 Issue: 03 Pages: 5924– 5930 (2023) ISSN: 0975-0290

Table 1. Comparison of the given work with previously published works.

Ref	Frequency (GHz)	Ant. Type	Bandwidth (%)	Gain(dB)	Layer	Method.
[16]	5.8	Microstrip	6.93	5.37	2	Metamaterial substrate
[17]	3.7-11.1	Microstrip	100	4.0-9.4	2	FSS substrate
[18]	10	-	31	19	2	Metamaterial superstrate
[19]	6-11	Microstrip	-	13.1	2	PRS and AMC
[20]	3-12.6	Microstrip	111.1	5-12.6	2	FSS substrate
[21]	2.45-5.8	Microstrip	-	4.69-6.45	2	FSS substrate
[23]	5.8	Microstrip	6.93	5.37	2	Metamaterial substrate
[32]	5.7	Microstrip	7.0	3.73	2	DNG metamaterial superstrate
[33]	2.4-5.8	Microstrip	-	6.4	1	Parasitic element
[34]	23.4-29.5	Microstrip	-	7	2	Metasurface
[35]	28	Microstrip	-	10	1	Array of metamaterial
[36]	5.3	Microstrip	5	9.5	1	DGS
[37]	34.5-45.5	Microstrip	-	15.5	2	MPLPM
[39]	3.7-4.1	Microstrip	-	8.51	2	H-shape DGS
[40]	2.332.57 2.91-4.53	Bow-tie	-	6.68-7.5	2	Metasurface DMS
Prop.	**8.4**	**Microstrip**	6.45	**6.5**	**1**	**Antenna and FSS are designed on a same substrate**

Metasurface, which are recognized for their remarkable electromagnetic characteristics. The suggested FSS is made up of a circular periodic structure with a rectangular stub in the center. It is highly stable across polarizations and incidence angles. The FSS operates on frequencies between 7 and 9 GHz. The FSS components are carefully placed around the two antennas on a regular basis to improve impedance matching, eliminate mutual coupling, and increase gain. The antenna's impedance bandwidth ranges from 8.0 to 8.55 GHz, and its isolation within the resonant band is 21 dB. At 8.4 GHz, the antenna has a maximum gain of 6.5 dB and a radiation efficiency of 77%. The ECC demonstrates extraordinary diversity performance with a value of 0.001, while the Diversity Gain (DG) reaches an astounding 10 dB. Instead of using separate substrates for the antenna and FSS, which consume quite a bit of space, the proposed method incorporates the antenna and FSS on a single substrate. This advancement enhances both performance and compactness, resulting in a more effective solution.

ACKNOWLEDGEMENTS

The authors grateful to the College of Electronic and Information Engineering, Nanjing University of Aeronautics and Astronautics (NUAA) for providing the necessary facilities, and in particular prof. Qunsheng Cao for supervising us.

REFERENCES

[1] Hussain, M.; Awan, W.A.; Ali, E.M.; Alzaidi, M.S.; Alsharef, M.; Elkamchouchi, D.H.; Alzahrani, A.; Fathy Abo Sree, M. ”Isolation Improvement of Parasitic Element-Loaded Dual-Band MIMO Antenna for Mm-Wave Applications. Micromachines”, 2022, 13, 1918.

[2] Bayarzaya, B.; Hussain, N.; Awan, W.A.; Sufian, M.A.; Abbas, A.; Choi, D.; Lee, J.; Kim, N. ”A Compact MIMO Antenna with Improved Isolation for ISM, Sub-6 GHz, and WLAN Application”. Micromachines. 2022, 13, 1355.

[3] Rahman, S. U, et al. ”Multifunctional polarization converting metasurface and its application to reduce the radar cross-section of an isolated MIMO antenna.” Journal of Physics D: Applied Physics, vol. 53, no. 30, pp. 305001, 2020.

[4] Khan, M.I, Khattak, M. I., Rahman, S. U., Qazi, A. B., Telba, A. A., and Sebak, A. Design and investigation of modern UWB-MIMO antenna with optimized isolation. Micromachines, vo. 11, no. 4, pp. 432, 2020.

[5] Ahmad, A., Ullah, A., Feng, C., Khan, M., Ashraf, S., Adnan, M., Nazir, S. and Khan, H.U., Towards an improved energy efficient and end-to-end secure protocol for iot healthcare applications. Security and Communication Networks, vol. 2020, pp.1-10, 2020.

[6] Hussain, N.; Awan, W. A.; Ali, W.; Naqvi, S. I.; Zaidi, A.; Le, T. T. ”Compact wideband patch antenna and its MIMO configuration for 28 GHz applications”. AEU Int J Electron Commun2021, 132, 153612.

[7] Ibrahim, A.A.; Abdalla, M.A.; Abdel-Rahman, A.B.; Hamed, H.F. ”Compact MIMO antenna with optimized mutual coupling reduction using DGS”. Int. J. Microw. Wirel. Technol., 2014, 6, 173–180.

[8] Ahmed M. A. Sabaawi Karrar Shakir Muttair Oras Ahmed Al-Ani Qusai Hadi Sultan , ”DualBand MIMO Antenna with Defected Ground Structure for Sub-6 GHz 5G Applications,” Progress In Electromagnetics Research C, Vol. 122, 57-66, 2022.

[9] G. Yan-Yun, L. Wang and Z. Zhang , ”The Novel Y Shaped Fractal Defected Ground Structure for the Mutual Coupling Reduction,” Progress In Electromagnetics Research M, Vol. 72, 13-21, 2018.

[10] Yang, Y.; Chu, Q.; Mao, C. ”Multiband MIMO antenna for GSM, DCS, and LTE indoor applications”. IEEE An-tennas Wirel. Propag. Lett., 2016, 15, 1573–1576.

[11] Sun Y, Tian M, Cheng GS. ”Characteristic Mode-Based Neutralization Line Design for MIMO Antenna”. In-ternational Journal of Antennas and Propagation. 2022 Jul 30;2022.

[12] OuYang, J.; Yang, F.; Wang, Z. ”Reducing mutual coupling of closely spaced microstrip MIMO antennas for WLAN application”. IEEE Antennas Wirel. Propag. Lett., 2011, 10, 310–313.

[13] Hussain, M.; Abbas, Q.; Gardzi, S. H. H.; Alibakhshikenari, M.; Falcone, F.; Limiti, E. ”Ultrawideband MIMO antenna realization for indoor Ka-band applications”. In 2022 United

States National Committee of URSI National Radio Science Meeting (USNC-URSI NRSM) (pp. 108109)., 2022.

[14] Saravanan, M.; Geo, V.B.; Umarani, S.M. ”Gain enhancement of patch antenna integrated with metamaterial inspired superstrate”. J Electr Sys Info Technol., 2018, 5, 263-270.

[15] Samantaray, D.; Bhattacharyya, S. ”A gain-enhanced slotted patch antenna using metasurface as superstrate configuration”. IEEE Transac Antennas Propag. 2020, 68, 6548-6556.

[16] Arnmanee, P.; Phongcharoenpanich, C. ”Improved microstrip antenna with HIS elements and FSS super-strate for 2.4 GHz band applications”. Int J Antennas Propag. 2018, 2018, 1-11.

[17] Kushwaha, N.; Kumar, R.; Oli, T. ”Design of a high-gain ultra-wideband slot antenna using frequency selec-tive surface”. Microwave Opt Technol Lett. 2014, 56, 1498-1502.

[18] Yuan, Y.; Xi, X.; Zhao, Y. ”Compact UWB FSS reflector for antenna gain enhancement”. IET Microwaves An-tennas Propag. 2019, 13, 1749-1755.

[19] Hsing-Yi, C.; Tao Y. ”Bandwidth enhancement of a U-slot patch antenna using dual-band frequency-selective surface with double rectangular ring elements”. Microwave Opt Technol Lett. 2011, 53, 1547-1553.

[20] Adelson, M.L.; Henrique, O.N.; Nilson, H.O.C; da-Silva, J.P. ”Effect of Metamaterial cells Array on a mi-crostrip patch antenna design”. J Microwaves Optoelectron Electromag Appl. 2020, 19, 327-342.

[21] Adibi, S.; Honarvar, M.A.; Lalbakhsh, A. ”Gain enhancement of wideband circularly polarized UWB antenna using FSS”. Radio Sci. 2021, 56, e2020RS007098.

[22] Afzal, M.U.; Lalbakhsh, A.; Esselle, K.P. ”Electromagnetic-wave beam-scanning antenna using near-field ro-tatable graded-dielectric plates”. J App Phy. 2018, 124, 234901–234911.

[23] Mackay, A.; Sanz-Izquierdo, B.; Parker, E.A. ”Evolution of frequency selective surfaces”. Forum for Electro-magnetic Research Methods and Application Technologies (FERMAT), Vol. 2, 1–7, 2014.

[24] Nair, R.U.; Jha, R.M. ”Electromagnetic design and performance analysis of airborne radomes: Trends and perspectives antenna applications corner”. Antennas Propag Mag. 2014, 56, 276–298.

[25] Luukkonen, O.; Costa, F.; Simovski, C.R.; Monorchio, A.; Tretyakov, S.A. ”A thin electromagnetic absorber for wide incidence angles and both polarizations”. IEEE Trans Antennas Propag. 2009, 57, 3119–3125.

[26] Zahirjoozdani, M.; Khalajamirhosseini, M.; Abdolali, A. ”Wideband radar cross-section reduction of patch array antenna with miniaturized hexagonal loop frequency selective surface”. Electron Lett. 2016, 52, 767–768.

[27] Hiranandani, M.A.; Yakovlev, A.B.; Kishk, A.A. ”Artificial magnetic conductors realized by frequen-cy-selective surfaces on a grounded dielectric slab for antenna applications”. IEEE Proc Microw Antennas Propag. 2006, 153, 487–493, 2006.

[28] Mark, R.; Rajak, N.; Mandal, K.; Das, S. ”Isolation and gain enhancement using metamaterialbased super-strate for MIMO applications”. Radioengineering 2019, 28(4), 689-695.

[29] Peng, H.; Zhi, R.; Yang, Q.; Cai, J.; Wan, Y.; Liu, G. ”Design of a MIMO antenna with high gain and enhanced isolation for WLAN applications”. Electron. 2021, 10(14), 1659.

[30] Jiang, H.; Si, L.M.; Hu, W.; Lv, X. ”A symmetrical dual-beam bowtie antenna with gain enhancement using metamaterial for 5G MIMO applications”. IEEE Photonics J. 2019, 11(1), 1-9.

[31] Lin, M.; Liu, P.; Guo, Z. ”Gain-enhanced Ka-band MIMO antennas based on the SIW corrugated technique”. IEEE Antennas Wirel Propag Lett. 2017, 16, 3084-3087.

[32] Nguyen, N.L. ”Gain enhancement for MIMO antenna using metamaterial structure”. Int J Microw Wirel Tech-nolo. 2019, 11(8), 851-862.

[33] Khajeh-Khalili, F.; Honarvar, M.A.; Naser-Moghadasi, M.; Dolatshahi, M. ”Gain enhancement and mutual coupling reduction of multiple-intput multiple-output antenna for millimeter-wave applications using two types of novel metamaterial structures”. Int J RF Microw Comp Aided Eng. 2020, 30(1), e22006.

[34] Firmansyah, T.; Herudin, H.; Suhendar, S.; Wiryadinata, R.; Santoso, M.I.; Denny, Y.R.; Supriyanto, T. ”Bandwidth and gain enhancement of MIMO antenna by using ring and circular parasitic with air-gap mi-crostrip structure”. TELKOMNIKA. 2017, 15(3), 1155-1163.

[35] . Niu, Z.; Zhang, H.; Chen, Q.; Zhong, T. ”Isolation enhancement in closely coupled dual-band MIMO patches antennas”. IEEE Antennas Wirel Propag Lett. 2019, 18(8), 1686-1690.

[36] Mohanty, A.; Behera, B. R.; Nasimuddin, N. ”Hybrid metasurface loaded tri-port compact antenna with gain enhancement and pattern diversity”. Int J RF Microw Comp Aided Eng. 2021, 31(11), e22795.

[37] Ullah, H.; Rahman, S.U.; Cao, Q.; Khan, I.; Ullah, H. ”Design of SWB MIMO antenna with extremely wide-band isolation”. Electron. 2020, 9(1), 194.

[38] Jabire, A.H.; Zheng, H.X.; Abdu, A.; Song, Z. ”Characteristic mode analysis and design of wide band MIMO antenna consisting of metamaterial unit cell”. Electron. 2019, 8(1), 68.

[39] Khan I, Zhang K, Wu Q, Ullah I, Ali L, Ullah H, Rahman SU. ”A Wideband High-Isolation Microstrip MIMO Circularly-Polarized Antenna Based on Parasitic Elements”. Materials. 2023 Jan;16(1):103.

[40] Rahman SU, Deng H, Sajjad M, Rauf A, Shafiq Z, Ahmad M, Iqbal S. ”Angularly stable frequency selective surface for the gain enhancement of isolated multiple input multiple output antenna”. Microwave and Optical Technology Letters. 2021 Nov;63(11):2803-10.

[41] Balanis, Constantine A. Antenna theory: analysis and design. John wiley & sons, 2016.

[42] Khan I, Wu Q, Ullah I, Rahman SU, Ullah H, Zhang K. ”Designed circularly polarized two-port microstrip MIMO antenna for WLAN applications”. Applied Sciences. 2022 Jan 20;12(3):1068.

[43] Qiu, Hongbing, Saeed Ur Rahman, and Habib Ullah. "A Compact SWB Monopole Antenna and FSS for." International Journal of Advanced Networking and Applications 14.6 (2023): 5658-5665.

[44] Khan, Imran, et al. "Compact Single Band Suppression Monopole Antenna for SWB Application." International Journal of Advanced Networking and Applications 14.5 (2023): 5645-5650.

[45] Ullah, Habib, Qunsheng Cao, Ijaz Khan, Saeed Ur Rahman, and Adamu Halilu Jabire. "A Novel Frequency Selective Surface Loaded MIMO Antenna with Low Mutual Coupling and Enhanced Gain." Progress In Electromagnetics Research M 118 (2023): 83-92.